Scalable Entanglement Certification via Quantum Communication

Pharnam Bakhshinezhad,[1,†,‡] Mohammad Mehboudi,[1] Carles Roch i Carceller,[2] and Armin Tavakoli[2,*]

[1]*Atominstitut, Technische Universität Wien, Stadionallee 2, 1020 Vienna, Austria*
[2]*Department of Physics and NanoLund, Lund University, Box 118, 22100 Lund, Sweden*

Harnessing the advantages of shared entanglement for sending quantum messages often requires the implementation of complex two-particle entangled measurements. We investigate entanglement advantages in protocols that use only the simplest two-particle measurements, namely, product measurements. For experiments in which only the dimension of the message is known, we show that robust entanglement advantages are possible but that they are fundamentally limited by Einstein-Podolsky-Rosen steering. Subsequently, we propose a natural extension of the standard scenario for these experiments and show that it circumvents this limitation. This leads us to prove entanglement advantages from every entangled two-qubit Werner state, evidence its generalization to high-dimensional systems, and establish a connection to quantum teleportation. Our results reveal the power of product measurements for generating quantum correlations in entanglement-assisted communication and they pave the way for practical semi-device-independent entanglement certification well beyond the constraints of Einstein-Podolsky-Rosen steering.

I. INTRODUCTION

Shared entanglement between a sender and a receiver that are connected over a quantum channel is the most powerful communication resource in quantum theory. This is famously showcased in the dense-coding protocol, where entanglement doubles the classical capacity of a noise-free qubit channel [1]. If the channel is used only once, which is the most pertinent scenario for experimental considerations, this entanglement-assisted prepare-and-measure (EAPM) scenario (see Fig. 1) can equally well be viewed as setting for efficient quantum communication and as a platform for semi-device-independent quantum information protocols. The latter is because the state, the sender, and the receiver are uncharacterized devices and only knowledge of the dimension of the channel is required to deduce the quantum nature of the correlations. In this

sense, the EAPM scenario offers an appealing path to certify the advantages of entanglement in experiments with limited characterization.

A central obstacle for harnessing entanglement advantages in the EAPM scenario is that protocols commonly need the receiver (Charlie) to measure both the particles, namely, the one coming from the entanglement source and the one arriving over the channel, in an entangled basis. In, e.g., optical systems, such measurements are well known to be impossible without extra photons or nonlinear effects [2–4], which can, e.g., limit experiments to using only single-photon carriers of multiple qubits (see e.g., Refs. [5,6]). In the EAPM scenario, for the simplest case of qubit systems, a series of dense-coding experiments have over time implemented increasingly sophisticated Bell basis measurements and thereby approached the theoretical limit of the entanglement advantage [7–14]. For systems of higher dimension than qubit, the situation is extra challenging. Even resolving one element of a high-dimensional entangled basis is impossible with ancilla-free linear optics [15]. The most high-dimensional optical Bell basis measurement hitherto realized is limited to three-level systems and uses ancillary photons [16,17]. In the EAPM scenario, this has led experiments based on high-dimensional entanglement and quantum communication to instead focus on simpler, suboptimal, measurements, compatible with standard linear optics [18]. The challenges associated with entangled measurements are broadly

---

*Corresponding author: armin.tavakoli@teorfys.lu.se
†Corresponding author: pharnam.bakhshinezhad@tuwien.ac.at
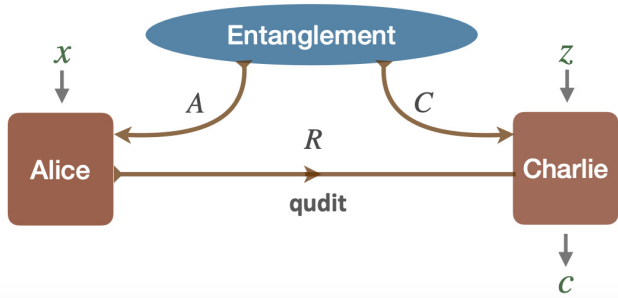‡P.B. previously published as Faraj Bakhshinezhad.

FIG. 1. The EAPM scenario between a sender (Alice) and a receiver (Charlie). The information, x, is encoded into one share of the entangled state.

relevant in the different correlation tests accommodated by the EAPM scenario [19–21].

However, while entangled measurements are provably necessary for the specific task of dense coding [22], this is not true in general. Interestingly, it has recently been shown that there exist well-known communication tasks that, in the EAPM scenario, admit their best implementation in protocols that rely only on the simplest joint measurements [23]. These are mere product measurements of the source and message particles; they therefore constitute the classical postprocessing of two completely separate single-particle measurements. In principle, this can greatly simplify the experiments, as the particles do not need to interfere with each other in the measurement device and can even be measured at separate times. Nevertheless, at present, little is known about how such protocols can be constructed. Moreover, another important aspect concerns the noise robustness of protocols based on product measurements. While entangled measurements are well known to reveal the correlation advantages of shared entanglement even from very noisy states [24,25], no counterpart is known for product measurements. That is, even though product measurements can sometimes be optimal under ideal conditions, their performance might deteriorate in the presence of significant amounts of noise in the entanglement distribution, rendering them unable to certify entanglement that is well within the reach of schemes that use entangled measurements. Indeed, certifying noisy forms of entanglement is a central matter for correlation experiments.

Here, we investigate entanglement advantages revealed by product measurements in the EAPM scenario and show that they are much more powerful than previously known. In all our scenarios, the source is fully untrusted. The operations of all the parties are also untrusted, up to the bounded dimension of the quantum communication channels. The paper is structured as follows. In Sec. II, we formalize the EAPM scenario. In Sec. III, we investigate high-dimensional entanglement by introducing concrete certification schemes in the EAPM scenario. We prove that the paradigmatic isotropic state is certified at noise rates well above the known thresholds for Bell nonlocality and closely resembling the thresholds known for Einstein-Podolsky-Rosen steering. In Sec. IV, we show that the results from Sec. III are actually close to optimal. This follows from a no-go result, in which we show that steering is a necessary condition for certifying entanglement advantages in any EAPM scenario with product measurements. In Sec. V, we set out to circumvent this fundamental limitation. We do so by considering a natural extension of the standard EAPM scenario, which we name the symmetric EAPM scenario. In the symmetric scenario, classical information is not only encoded in one share of the state (Alice, in Fig. 1) but in both shares of the state (see Fig. 2). For qubit systems, we prove that every entangled Werner state implies an advantage. Finally, in Sec. VI, we introduce a prime-dimensional generalization of the scheme in Sec. V. We present evidence, on the basis of which we argue that every state supporting fidelity-based quantum teleportation can be certified. This notably includes every entangled isotropic state.

II. THE EAPM SCENARIO

The EAPM scenario is illustrated in Fig. 1. Alice and Charlie share a state ρ_{AC}, which can have an arbitrary local dimension. Alice selects a classical input x and encodes it on her share of the state via a completely positive trace-preserving (CPTP) map, $\Lambda_x^{A \to R}$, the output system, R, of which, here called the message, has a known dimension d. The total state arriving at Charlie becomes

$$\tau_x^{RC} = (\Lambda_x^{A \to R} \otimes \mathbb{1}^C)[\rho_{AC}]. \quad (1)$$

Finally, Charlie selects a classical input z and performs a joint quantum measurement $\{M_{c|z}^{RC}\}$ with outcome c. The Born rule gives the quantum correlations, $p(c|x,z) = \text{tr}(\tau_x^{RC} M_{c|z})$. Note that the set of states $\{\tau_x^{RC}\}$ realizable via arbitrary CPTP maps for Alice and an arbitrary initial entangled state can be completely characterized as τ_x^{RC} being a $d \times D$ dimensional bipartite state with $\text{tr}_R(\tau_x^{RC}) = \tau^C$, where τ^C is the reduced state, which is notably independent of x. Note that D is the dimension of the source particle, which can be arbitrary.

Our focus is on protocols where Charlie's measurements act separately on systems R and C. This can be a product measurement followed by a classical postprocessing of the respective outcomes, i.e.,

$$M_{c|z}^{RC} = \sum_{c_1, c_2} p(c|c_1, c_2) N_{c_1|z}^R \otimes N_{c_2|z}^C, \quad (2)$$

where $\{N_{c_1|z}^R\}$ and $\{N_{c_2|z}^C\}$ are single-system measurements and $p(c|c_1, c_2)$ is some (perhaps stochastic) rule for deciding the final outcome c from the local outcomes (c_1, c_2).

More generally, the measurements can also be adaptive [22], i.e., Charlie could use the outcome on system R to inform his measurement on system C and vice versa. These adaptive product measurements take the form $M_{c|z}^{RC} = \sum_{c_1,c_2} p(c|c_1,c_2) N_{c_1|z}^R \otimes N_{c_2|z,c_1}^C$ and $M_{c|z}^{RC} = \sum_{c_1,c_2} p(c|c_1,c_2) N_{c_1|z,c_2}^R \otimes N_{c_2|z}^C$, respectively.

We are interested in comparing the correlations, $p(c|x,z)$, obtained from shared entanglement and product measurements, with those obtained without shared entanglement. The latter correspond to standard (entanglement-unassisted) quantum prepare-and-measure scenarios, i.e., Alice can send any d-dimensional state α_x to Charlie, who can perform an arbitrary quantum measurement on it,

$$p(c|x,z) = \operatorname{tr}\left(\alpha_x M_{c|z}\right). \tag{3}$$

Shared classical randomness is additionally permitted between the parties.

III. CERTIFYING HIGH-DIMENSIONAL ENTANGLEMENT IN THE EAPM SCENARIO

We begin by identifying a scheme in the EAPM scenario that enables us to certify entanglement under substantial and dimension-scalable noise rates. To this end, consider the following scheme. Let Alice have an input $x \equiv (x_0, x_1) \in \{0, \ldots, d-1\}^2$ and let Charlie have an input $z \in \{0, \ldots, d\}$, where d is a prime number. The parties have the objective of computing (via the output c), for each z, a specific binary function of x. These functions are

$$\begin{aligned} z \neq d : \quad & w_z = x_1 - 2zx_0 \mod d, \\ z = d : \quad & w_d = x_0. \end{aligned} \tag{4}$$

The average success probability of computing the functions is therefore

$$\mathcal{S}_d = \frac{1}{d^2(d+1)} \sum_{x,z} p(c = w_z | x, z). \tag{5}$$

Next, we will analyze $\mathcal{S}_d$ in a quantum setting with and without entanglement and prove that it certifies entanglement under product measurements.

A. Protocol with shared entanglement and product measurements

Now consider a specific quantum protocol based on shared entanglement and product measurements. Let the shared state be $\rho_{AC} = \phi_d^+$, where $\phi_d^+ = |\phi_d^+\rangle\langle\phi_d^+|$ is the maximally entangled state, $|\phi_d^+\rangle = (1/\sqrt{d})\sum_{i=0}^{d-1}|ii\rangle$. Next, define the clock and shift operators $Z = \sum_{k=0}^{d-1} e^{(2\pi ik/d)}|k\rangle\langle k|$ and $X = \sum_{k=0}^{d-1}|k+1\rangle\langle k|$, where $k+1$ is

computed modulo d. Choose Alice's CPTP maps, Λ_x, as corresponding to the unitaries

$$U_x = X^{x_0}Z^{x_1}. \tag{6}$$

Note that for the special case of $d = 2$, X and Z are simply two of the Pauli operators and U_x is effectively the four Pauli rotations. Finally, we must select Charlie's product measurements. For the special case of $d = 2$, we choose them as products of the three Pauli observables, namely,

$$E_0 = X \otimes X, \qquad E_1 = Z \otimes Z, \quad \text{and} \quad E_2 = XZ \otimes XZ, \tag{7}$$

with $M_{c|z} = \frac{1}{2}(\mathbb{1} + (-1)^c E_z)$. Beyond dimension two, following Eq. (2), we define the measurements as the postprocessing of the outcomes obtained in two separate basis measurements of systems R and C, respectively,

$$M_{c|z} = \sum_{c_1,c_2=0}^{d-1} |e_{c_1,z}\rangle\langle e_{c_1,z}| \otimes |e_{c_2,z}^*\rangle\langle e_{c_2,z}^*| \delta_{c_1-c_2,c}, \tag{8}$$

where the asterisk $(*)$ denotes complex conjugation and the addition in $\delta_{c_1-c_2,c}$ is taken modulo d. Notably, in odd-prime dimensions, the local bases $\{|e_{m,z}\rangle\}$ are mutually unbiased. These are known to admit the form $|e_{m,d}\rangle = |m\rangle$ and $|e_{m,z}\rangle = (1/\sqrt{d})\sum_{l=0}^{d-1}\omega^{l(m+zl)}|l\rangle$ for $z \neq d$, where $\omega = e^{(2\pi i/d)}$ [26]. The unbiasedness property is not *de facto* necessary for the success of the protocol but is a convenient choice.

In order to evaluate the average success probability in Eq. (5), it is handy to first identify the following relations, which can be straightforwardly verified:

$$\begin{aligned} X^t|e_{m,z}\rangle &= \omega^{zt^2-tm}|e_{m-2zt,z}\rangle, \\ Z^t|e_{m,z}\rangle &= |e_{m+t,z}\rangle, \\ X^t|e_{m,z}^*\rangle &= \omega^{-zt^2+tm}|e_{m-2zt,z}^*\rangle, \\ Z^t|e_{m,z}^*\rangle &= |e_{m-t,z}^*\rangle, \end{aligned} \tag{9}$$

valid for $z \neq d$ and integer t. Using these, one straightforwardly finds that each of the functions is computed deterministically: i.e., $p(c|x,z) = \delta_{c,w_z}$, leading to $\mathcal{S}_d = 1$.

B. Bounding protocols without shared entanglement

Next, we must determine a useful bound $\mathcal{S}_d \leq L_d$ valid for any quantum strategy without shared entanglement. Since this corresponds to bounding the expression in Eq. (5) in a standard quantum prepare-and-measure scenario, the correlations are given by Eq. (3). The relevant

quantity becomes

$$\max_{\{\alpha_x\},\{M_{c|z}\}} \frac{1}{d^2(d+1)} \sum_{x,z} \text{tr}\left(\alpha_x M_{w_z|z}\right), \quad (10)$$

where α_x is a d-dimensional state. We restrict the analysis to prime-number dimensions because in these cases, the conditions in Eq. (4) are particularly hard to meet without entanglement. The task at hand can be seen as an (unorthodox) variant of a quantum random access code [27,28]. The proof ideas recently developed for quantum random access codes in Ref. [29] can be immediately modified to obtain a general bound, L_d, on Eq. (10), namely,

$$L_d = \frac{1}{d}\left(1 + \frac{d-1}{\sqrt{d+1}}\right), \quad (11)$$

for prime d. The derivation is detailed in Appendix A and is based on analyzing operator norms for sums of the measurement operators. Regardless of the protocol used, the observation of $\mathcal{S}_d > L_d$ implies the certification of entanglement. The bound L_d is typically not tight (except for $d = 2$), i.e., it does not equal the value defined in Eq. (10). The reason for this becomes apparent in Appendix A, where both operator-norm inequalities and concavity inequalities are employed, the saturation of which is not guaranteed in general. Nevertheless, to give an indication of how close to optimal the bound is, we have numerically optimized the argument in Eq. (10) over the set of quantum states and measurements. For $d = 3, 5, 7$, we obtain the lower bounds 0.6616, 0.5121, and 0.4233 respectively, which can be compared to the upper bounds 0.6667, 0.5266, and 0.4459 obtained, respectively, from Eq. (11). We note that numerical techniques likely can be used to improve the bound in Eq. (11) but only for specific values of d [30].

Even though the bound in Eq. (11) is not generally tight, it is good enough to reveal the qualitative abilities of product measurements in a dimension-scalable manner. To showcase that, we focus on the seminal isotropic state,

$$\rho_v^{\text{iso}} = v\phi_d^+ + \frac{1-v}{d^2}\mathbb{1}, \quad (12)$$

with visibility $v \in [0, 1]$. Thus, when running the strategy from the previous section, we compute the smallest visibility for which the state produces a value of $\mathcal{S}_d$ that exceeds the limit in Eq. (11). For comparison, the isotropic state is known to be entangled if and only if $v > (1/(d+1))$ [31].

Corollary 1. For every prime dimension d, entanglement certification in the EAPM scenario with product measurements is possible for the isotropic state when

$$v > \frac{1}{\sqrt{d+1}}. \quad (13)$$

This exhibits an inverse-square-root scaling in the dimension parameter, thus showing that product measurements become increasingly good at certifying the entanglement. In particular, for $d = 2$, it reduces to $v > 1/\sqrt{3}$, which significantly improves on previous protocols [23] and happens to equal the exact threshold for steerability of ρ_v^{iso} for the same number (three) of measurements [32]. Moreover, for prime d, Eq. (13) exactly matches the bound for steerability of ρ_v^{iso} under $d + 1$ mutually unbiased bases obtained from the steering inequality of Ref. [33].

IV. NO ENTANGLEMENT ADVANTAGE WITHOUT STEERING

It is not a coincidence that our above scheme happens to give critical visibilities that closely parallel results known for steering. As we now show, the above results are examples of saturation (or near saturation) of a more fundamental limitation that applies to any protocol in the EAPM scenario using adaptive product measurements.

Proposition 1. Let ρ_{AC} be any entangled state that is not steerable from C to A. Then, any probability distribution in the EAPM scenario obtained from adaptive product measurements can be simulated in a quantum model with shared classical randomness.

Proof. Consider first product measurements that are adaptive from system C to system R. The probability distribution can then be written

$$p(c|x, z) = \sum_{c_1,c_2} p(c|c_1, c_2)\text{Tr}\left(\Lambda_x[\rho_{c_2|z}]M_{c_1|z,c_2}^R\right), \quad (14)$$

where $\rho_{c_2|z} = \text{Tr}_C\left(\mathbb{1} \otimes M_{c_2|z}^C \rho_{AC}\right)$ are the unnormalized states remotely prepared on A by measuring C. If ρ_{AC} is unsteerable from C to A, there exists a local hidden-state decomposition $\rho_{c_2|z} = \sum_\lambda p(\lambda)p(c_2|z,\lambda)\tau_\lambda$ for some arbitrary-dimensional quantum states $\{\tau_\lambda\}$. Inserting this, we obtain

$$p(c|x, z) = \sum_{\lambda,c_1,c_2} p(\lambda)p(c|c_1, c_2)p(c_2|z, \lambda)$$
$$\times \text{Tr}\left(\Lambda_x[\tau_\lambda]M_{c_1|z,c_2}^R\right). \quad (15)$$

This can be simulated without entanglement as follows. Let Alice and Charlie share λ, with distribution $p(\lambda)$. Alice prepares τ_λ and applies Λ_x to it, sending the d-dimensional state $\Lambda_x[\tau_\lambda]$ to Charlie. He draws c_2 from the distribution $p(c_2|z, \lambda)$, then applies the measurement $\{M_{c_1|z,c_2}^R\}$, and lastly draws c from $p(c|c_1, c_2)$. This reproduces the distribution in Eq. (15).

The case of product measurements adaptive from system R to system C is similarly treated. The probability

distribution becomes

$$p(c|x,z) = \sum_{c_1,c_2} p(c|c_1,c_2) \text{Tr}\left(\Lambda_x[\rho_{c_2|z,c_1}]M_{c_1|z}^R\right), \quad (16)$$

where $\rho_{c_2|z,c_1} = \text{Tr}_C\left(\mathbb{1} \otimes M_{c_2|z,c_1}^C \rho_{AC}\right)$ are the unnormalized states remotely prepared on A. The existence of a local hidden-state model implies

$$p(c|x,z) = \sum_{\lambda,c_1,c_2} p(\lambda)p(c|c_1,c_2)p(c_2|z,c_1,\lambda)$$
$$\times \text{Tr}\left(\Lambda_x[\tau_\lambda]M_{c_1|z}^R\right). \quad (17)$$

To simulate this distribution without entanglement, one distributes λ and lets Alice prepare τ_λ and run it through the map Λ_x. Charlie first measures the message, then uses the outcome c_1 to draw c_2 from $p(c_2|z,c_1,\lambda)$, and finally draws c from $p(c|c_1,c_2)$. ∎

A noteworthy corollary of this argument is that for product measurements adaptive from C to R, in an EAPM scenario with N inputs for Charlie, one-way steerability under just N measurements is necessary for an entanglement advantage. This makes a significant difference, since steerability under a limited number of measurements is known to be considerably more constrained than steerability under unboundedly many measurements [32]. In view of this, the scheme from Sec. III, which has led to Corollary 1 via independent product measurements, is optimal for $d = 2$, since it coincides with the steering bound of ρ_v^{iso} under three measurements. For larger d, it is unlikely that our result from the previous section can be much improved, because of the steering results for $N = d + 1$ bases in [33,34]. However, by employing potentially unboundedly many measurements (instead of $d + 1$ as in our case), it may be possible to approach the ultimate steering limit [35] on the parameter v.

Proposition 1 provides a fundamental limitation on the abilities of product measurements in the EAPM scenario. Although we have already found that significantly noise-tolerant entanglement certification is possible, it is impossible to certify any state that is entangled but not steerable. Therefore, in what follows, we go beyond the EAPM scenario to show that this obstacle can be overcome, allowing for even stronger entanglement certification.

V. THE SYMMETRIC EAPM SCENARIO

In order to circumvent the limitation on product-measurement schemes imposed by Proposition 1, we consider an extended version [24,36] of the original EAPM scenario, which we refer to as the symmetric EAPM scenario. The extension is modest in terms of an implementation perspective and is conceptually natural. In the original

EAPM scenario, classical information is only encoded into half the entangled state—namely, by Alice—into system A. In the symmetric EAPM scenario, we also want to encode classical information in the other half of the entangled state. To make this possible, we add a third party, Bob, who selects an input y and encodes it into the second source particle before relaying it to Charlie (see Fig. 2).

Let us now write the state as ρ_{AB}, distributed to Alice and Bob. They each select x and y and perform CPTP maps $\Lambda_x^{A \to R_1}$ and $\Gamma_y^{B \to R_2}$, with the output systems R_1 and R_2 each being of dimension d. These are now separate, but potentially entangled, messages. Charlie's measurements, $\{M_{c|z}^{R_1R_2}\}$, are applied jointly to both messages, leading to the quantum correlations

$$p(c|x,y,z) = \text{tr}\left((\Lambda_x^{A \to R_1} \otimes \Gamma_y^{B \to R_2})[\rho_{AB}]M_{c|z}^{R_1R_2}\right). \quad (18)$$

We remark that all parties can also share classical randomness, which can be included in the state ρ_{AB}.

Again, we are interested in how protocols using shared entanglement and product measurements can outperform protocols using no shared entanglement. The correlations from the latter are described as

$$p(c|x,y,z) = \text{tr}\left(\alpha_x \otimes \beta_y M_{c|z}\right), \quad (19)$$

where α_x and β_y are d-dimensional states sent from Alice and Bob, respectively, to Charlie. Note that in contrast to the original EAPM scenario, the measurement $\{M_{c|z}\}$ can now be entangled.

A direct inspection shows that the argument used to arrive at Proposition 1 cannot be repeated for the symmetric EAPM scenario. Indeed, the argument relies on the fact that Alice's operations do not influence the other particle, making one-way steering relevant. The counterparts to these states arriving to Charlie are now influenced by Bob. We shall see that this is not a superficial observation; the symmetric EAPM scenario can indeed certify unsteerable
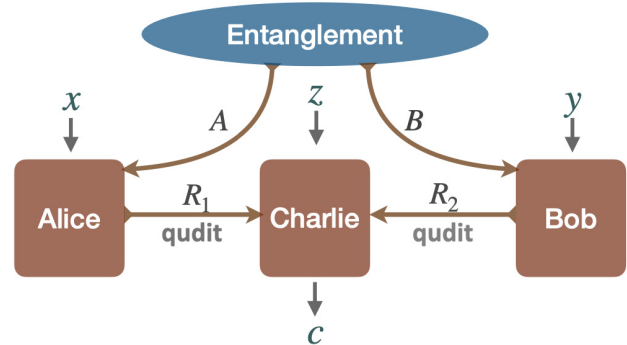

FIG. 2. The symmetric EAPM scenario between the senders (Alice and Bob) and the receiver (Charlie). The information, (x,y), is encoded into the shares of the entangled state.

entanglement. To show this, let us focus on qubit systems and the following scheme.

Alice and Bob each select two bits, $x \in (x_0, x_1) \in \{0, 1\}^2$ and $y \in (y_0, y_1) \in \{0, 1\}^2$. Charlie selects one of three inputs $z \in \{0, 1, 2\}$, each with binary outputs $c \in \{0, 1\}$. The aim is for Charlie to compute a binary function for each z; specifically, the functions

$$
\begin{aligned}
z = 0 : & \quad w_0 = x_0 + y_0, \\
z = 1 : & \quad w_1 = x_1 + y_1, \\
z = 2 : & \quad w_2 = x_0 + x_1 + y_0 + y_1,
\end{aligned}
\tag{20}
$$

computed modulo 2. The average success probability becomes

$$
\mathcal{R}_2 = \frac{1}{48} \sum_{x,y,z} p(c = w_z | x, y, z).
\tag{21}
$$

In analogy with the discussion in Sec. III, this task can be performed deterministically with shared entanglement and product measurements. In complete analogy with the protocol in Sec. III, we let $\rho_{AB} = \phi_2^+$ and we let Charlie perform the separate Pauli observables in Eq. (7). Alice and Bob both select among the same four Pauli unitaries, namely, U_x and U_y, as given in Eq. (6). Evaluating Eq. (21) then gives $\mathcal{R}_2 = 1$.

The key question is to determine the largest value of $\mathcal{R}_2$ achievable in a quantum model without shared entanglement. Consider first a classical protocol, in which α_x and β_y in Eq. (19) are all diagonal in the same basis. An optimal strategy is for Alice and Bob to simply send x_0 and y_0, respectively, leading to a deterministic output for $z = 0$ but random outputs for $z \in \{1, 2\}$ and thus a value of $\mathcal{R}_2 = \frac{2}{3}$. We prove in Appendix B that this cannot be improved in a generic quantum protocol without shared entanglement, i.e., any model of the form Eq. (19) obeys $\mathcal{R}_2 \leq \frac{2}{3}$. Consequently, any quantum over classical advantage in the scheme must be due to entanglement. Notably, the same is not true for the scheme presented in Sec. III; there, the classical limit can be overcome using quantum communication without entanglement and can then be further enhanced by adding entanglement.

We remark that the proof presented in Appendix B applies more generally. It can be used to bound the average success probability in any input-output scenario in which Charlie has binary outputs and the winning conditions are XOR between balanced functions of Alice's input and Bob's input. Nevertheless, we focus on the specific case in Eq. (20) because of its relevance for certifying the entanglement of isotropic states [37]. Indeed, a simple calculation now shows that every entangled isotropic state is certified, i.e., $\mathcal{R}_2 > \frac{2}{3}$ when $v > \frac{1}{3}$. In contrast, the state is steerable under generic projective measurements only when $v > \frac{1}{2}$ [35]. Notably, this result completely solves the main open problem raised in Ref. [23].

More generally, consider the so-called maximally entangled fraction of ρ_{AC},

$$
\mathrm{EF}_d(\rho) = \max_{\Lambda_1, \Lambda_2} \langle \phi_d^+ | (\Lambda_1 \otimes \Lambda_2)[\rho] | \phi_d^+ \rangle,
\tag{22}
$$

where Λ_1 and Λ_2 are CPTP maps with d-dimensional output spaces. A nontrivial maximally entangled fraction corresponds to $\mathrm{EF}_d(\rho) > \frac{1}{d}$ and is the key parameter for quantifying fidelity-based quantum teleportation [38]. We find that it gives a sufficient condition for whether a state can be certified via product measurements in our scheme.

Proposition 2. Every state ρ_{AB} with a nontrivial qubit maximally entangled fraction can be certified in the symmetric EAPM scenario using product measurements. In particular, it can achieve the value

$$
\mathcal{R}_2 = \frac{1}{3} + \frac{2}{3} \mathrm{EF}_2(\rho_{AB}).
\tag{23}
$$

Moreover, this value is optimal when ρ_{AB} is a pure two-qubit state.

Proof. Here, we show only that Eq. (23) is attainable, with remaining details given in Appendix C. Upon receiving the shares of ρ_{AC}, let Alice and Bob first apply some arbitrary CPTP maps Λ_1 and Λ_2, respectively, the output systems of which are d-dimensional. Subsequently, they each implement the previously given protocol, i.e., they perform unitaries U_x and U_y, respectively, and Charlie measures the observables in Eq. (7). We can express the average success probability as

$$
\mathcal{R}_2 = \frac{1}{2} + \frac{1}{96} \mathrm{tr} \left((\Lambda_1 \otimes \Lambda_2)[\rho] \sum_z \mathcal{B}_z^{(1)} \otimes \mathcal{B}_z^{(2)} \right),
\tag{24}
$$

where

$$
\begin{aligned}
\mathcal{B}_0^{(1)} &= \sum_x (-1)^{x_0} U_x^\dagger X U_x = 4X, \\
\mathcal{B}_1^{(1)} &= \sum_x (-1)^{x_1} U_x^\dagger Z U_x = 4Z, \\
\mathcal{B}_2^{(1)} &= \sum_x (-1)^{x_0 + x_1} U_x^\dagger X Z U_x = 4XZ.
\end{aligned}
\tag{25}
$$

The right-hand sides are obtained after some simplifications. Due to the symmetry of the protocol, we have $\mathcal{B}_z^{(1)} = \mathcal{B}_z^{(2)}$. One then observes that

$$
\sum_z \mathcal{B}_z^{(1)} \otimes \mathcal{B}_z^{(2)} = 16(4\phi_2^+ - \mathbb{1}).
\tag{26}
$$

Upon insertion into Eq. (24) and allowing for an optimization over the channels Λ_1 and Λ_2, we obtain Eq. (23). ∎

Thus, the usefulness of a state in teleportation is a sufficient condition for certification in the symmetric EAPM scenario. Notably, many states with a nontrivial maximally entangled fraction do not admit any steering. The most immediate example is the isotropic state in the interval $\frac{1}{3} < v < \frac{1}{2}$ [35]. We remark that we have numerically explored the trade-off between $\mathcal{R}_2$ and the set of (mixed) two-qubit states with a bounded maximally entangled fraction and we again find that Eq. (23) is the optimal value of $\mathcal{R}_2$ for every such state.

VI. TOWARD HIGH-DIMENSIONAL SCHEMES

Having found that the symmetric EAPM scenario can for some classes of states enable even optimal entanglement advantages under product measurements, we proceed with investigating whether the same is also possible for high-dimensional systems. To this end, we draw inspiration from the scheme in Sec. III and extend it to the symmetric EAPM scenario.

Let d be an odd prime number. Let Alice and Bob each select one of d^2 inputs, $x = (x_0, x_1) \in \{0, \ldots, d-1\}^2$ and $y = (y_0, y_1) \in \{0, \ldots, d-1\}^2$. Charlie selects $z \in \{0, \ldots, d\}$ and outputs $c \in \{0, \ldots, d-1\}$. The winning conditions correspond to computing the following functions:

$$
\begin{aligned}
z \neq d : \quad & w_z = x_1 + y_1 - 2z(x_0 - y_0) \quad \mod d, \\
z = d : \quad & w_d = x_0 - y_0 \quad \mod d.
\end{aligned}
\tag{27}
$$

The average success probability of computing these functions is

$$
\mathcal{R}_d = \frac{1}{d^4(d+1)} \sum_{x,y,z} p(c = w_z | x, y, z). \tag{28}
$$

Note that for $d = 2$, this reduces to the qubit scheme from Sec. V.

A protocol based on product measurements, analogous to that used in Sec. III, can deterministically compute each of the winning functions. That is, choose $\rho_{AB} = \phi_d^+$, choose Alice's and Bob's unitaries as in Eq. (6), and choose Charlie's measurements as in Eq. (8), with the $d + 1$ mutually unbiased bases $\{|e_{m_z}\rangle\}$. One then calculates that $\mathcal{R}_d = 1$.

Now consider a fully classical model. A simple protocol, just like that for $\mathcal{R}_2$, is to send, e.g., x_0 and y_0 to Charlie and thus let him output correctly ($c = w_z$) when $z = d$ but output at random when $z \neq d$. This leads to $\mathcal{R}_d = 2/(d+1)$. One may wonder whether there exist a quantum strategy without entanglement that improves this bound. Nonetheless, in analogy with what has been proven for the qubit case in Sec. V, we are unable to find any such protocol. In particular, when employing the strategy mentioned above,

that was optimal for shared entanglement, but now to the case without shared entanglement, we obtain the classical score $\mathcal{R}_d = 2/(d+1)$ (for more details, see Appendix D). While for $d = 2$ we have proved analytically that the bound cannot be improved, in Appendix B, for the cases of $d = 3$ and $d = 5$, we have used a numerical search based on the see-saw method [39] to optimize $\mathcal{R}_d$ over the operations of Alice, Bob, and Charlie without shared entanglement. Specifically, we optimize $\mathcal{R}_d$ in Eq. (28) for all possible correlations according to Eq. (19) for any set of local quantum states α_x and β_y in Alice's and Bob's laboratories, respectively, and measurements $M_{c|z}$ in Charlie's laboratory. The optimization is rendered as a semidefinite program with variables iterating in a see-saw manner [40]. That is, we begin sampling random quantum states α_x and β_y with dimension d and optimize $\mathcal{R}_d$ for any of Charlie's measurements $M_{c|z}$. The optimal $M_{c|z}$ are stored and $\mathcal{R}_d$ is again optimized but now over all of Alice's possible states α_x. Again, the optimal α_x are stored and now the optimization runs over all of Bob's possible states β_y. This routine of three separate optimizations is then repeated until the estimated value of $\mathcal{R}_d$ converges (within a precision factor of 10^{-4}). In over 300 separate trials for each d, we have without exception found that the obtained value of $\mathcal{R}_d$ coincides with the classical bound. On this basis, we make the following conjecture.

Conjecture 1. For every odd prime d, the largest average success probability achievable in a quantum model without shared entanglement is

$$
\mathcal{R}_d = \frac{2}{d+1}. \tag{29}
$$

Interestingly, if the conjecture is true, it implies that the strong-entanglement advantages previously proven for qubit systems can be extended to high-dimensional systems. In Appendix D, we prove that the connection between the maximally entangled fraction and the average success probability, seen in Proposition 2, generalizes to larger d.

Proposition 3. For every odd prime d and state ρ_{AB}, there exists a quantum model achieving the average success probability

$$
\mathcal{R}_d = \frac{1}{d+1} + \frac{d}{d+1} \mathrm{EF}_d(\rho). \tag{30}
$$

Moreover, the numerics for $d = 3$ suggest that for pure states the value in Eq. (30) is optimal but reveals that the same is not always true for mixed states. If Conjecture 1 is true, Proposition 3 implies that every state with a nontrivial maximally entangled fraction exceeds the limitation of Eq. (29) and is therefore certified as entangled. In particular, every entangled isotropic state ρ_v^{iso} has a nontrivial

maximally entangled fraction and therefore this family of states is optimally certified.

VII. DISCUSSION

We have shown that product measurements are sufficient for revealing the advantages of noisy forms of entanglement in prepare-and-measure scenarios and that this can be achieved via simple communication tasks. In the standard EAPM scenario, we have shown that visibility requirements for white noise can decrease as the inverse square root of the dimension. However, we have also shown that this scalability is fundamentally limited by a need for steerability for entanglement advantages. By proposing the symmetric EAPM scenario, we have shown how this limitation can be overcome, sometimes even in an optimal way. This is exemplified by every entangled-qubit Werner state being certified, as well as every state useful for fidelity-based teleportation. Beyond qubits in the symmetric EAPM scenario, we have also shown how these results can be generalized to prime-dimensional systems but this ultimately requires a proof of Conjecture 1. Extending our methods to arbitrary nonprime dimensions is a natural next step.

Our results pave the way for theoretical exploration and experimental implementation of strong forms of semi-device-independent entanglement certification, which may apply also to finer entanglement concepts such as Schmidt numbers or fidelity estimation with a target state. It is appropriate to label our scenarios as semi-device-independent, because they require none of the quantum devices to be perfectly characterized but *only* that the number of degrees of freedom in the channel is bounded. Therefore, this form of entanglement certification is far

stronger than standard entanglement witnessing, where the devices are assumed to be flawless. For instance, the latter is known to be vulnerable to false positives when devices do not precisely correspond to the desired measurement [41–43].

The main results of this work are summarized in the first two rows of Table I and the rest of the table compares our results with other relevant types of protocols. The table focuses on the well-known isotropic state for the sake of simplicity and to provide a concrete benchmark for the protocols. However, in general, our results apply to arbitrary states, as no assumption on the entanglement source is required. Using Table I, we now proceed to discuss our results in this broader context of entanglement certification.

First, in Table I it is shown that our protocol for the EAPM scenario, which is based on measuring products of complete sets of MUBs, has the same certification performance as steering protocols based on complete sets of MUBs [33,45]; at least, when one uses the best-known closed expression for the performance of the two protocols. However, the exact performance of both protocols is underestimated, since a precise analytical solution is not known in both cases. Notably, if one considers general steering protocols, with infinitely many measurements, the critical visibility can be further reduced [35]. It is an interesting conceptual question whether there exist product-measurement protocols in the EAPM scenario that, in the limit of many measurements, can reach the critical visibility for steering, which is $v = (H_d - 1)/(d - 1)$, where $H_d = \sum_{k=1}^{d} 1/k$. However, our protocols in the symmetric EAPM scenario, again using products of complete sets of MUBs, significantly outperform the general steering bound. Due to our use of product measurements, we

TABLE I. A summary of the results and a comparison with other approaches. The "Qubit" and "Qudit" columns indicate bounds on the critical visibility for certifying the isotropic state. In the case of the symmetric EAPM scenario (also dense coding and general steering), the results are optimal. In the case of *Qubit Bell nonlocality*, the result is known to be nearly optimal [44] but for *Qudit Bell nonlocality*, the optimal bound is largely an open problem. We have included a comparison with the best-known steering bound for protocols based on complete sets of mutually unbiased bases, since our construction in the EAPM scenario also is based on these bases. The colored box assumes Conjecture 1. Proposition 1 shows a fundamental limitation in the EAPM scenario. Whether a corresponding limitation exists in the symmetric EAPM scenario is an open problem but it must be an entanglement concept that is weaker than usefulness in fidelity-based quantum teleportation.

	Qubit	Qudit	Fundamental limitation
EAPM	$v > (1/\sqrt{3})$	$v > (1/\sqrt{d+1})$	One-way steering
Symmetric EAPM	$v > \dfrac{1}{3}$	$v > (1/(d+1))$	?
Steering (via MUBs)	$v > \dfrac{1}{3}$	$v > (1/\sqrt{d+1})$ [33,45]	Number of MUBs
Steering (general)	$v > \dfrac{1}{2}$	$v > [(H_d - 1)/(d - 1)]$ [35]	Local hidden states
Dense coding	$v > \dfrac{1}{3}$	$v > (1/(d+1))$	Bell-state measurement
Bell nonlocality	$v > 0.6961$ [44]	$v > 0.6734$ [46] for $d \to \infty$	Local hidden variables

achieve this while using similar experimental resources as employed in steering experiments. Interestingly, from the point of view of the assumptions made on the system, we require only a dimension bound on the channel, which is often less severe than the assumption that one measurement device is flawlessly characterized, which is employed in steering. Notably, a strict dimension assumption can also be relaxed so that undesired small high-dimensional components associated with the implementation can be taken into account [47].

Second, it is well known that d-dimensional dense-coding protocols can detect every isotropic entangled state, namely, $v > (1/(d + 1))$ [24]. As we have proved for qubits and conjectured for higher dimensions, the same holds for our protocol in the symmetric EAPM scenario. In this sense, we preserve the certification power for the isotropic state while greatly reducing the experimental requirements; from deterministic and complete Bell-state measurements to product measurements of separate systems. It is relevant to note that we are not the first to realize that product measurements can give rise to strong quantum correlations in the EAPM scenario, as this has been reported in Ref. [23]. However, the protocol proposed there works only for qubits and while it is optimally implemented with product measurements, it has a very small noise tolerance. Specifically, it achieves $v = 1/\sqrt{2} \approx 0.7071$, compared to our $v = 1/\sqrt{3} \approx 0.5774$ in the EAPM scenario and $v = 1/3$ in the symmetric EAPM scenario. Note that the assumptions in these protocols are always the same, namely, a dimension bound on the channel.

Third, we can compare our certification results to those obtained in Bell-inequality tests. Certification via nonlocality is conceptually the strongest, since it requires no assumptions beyond the validity of quantum theory but the certification performance is more limited. Little is known about the possibility of violating Bell inequalities with isotropic states beyond dimension two. To our knowledge, the best bound on v is that reported in Ref. [46]; it decreases monotonically with d but converges only to $v = 0.6734$ in the limit of large d. A more certain comparison is possible in the qubit case; here, the optimal known visibility is $v \approx 0.6961$ and is known that no Bell inequality can reduce it below $v \approx 0.6875$ [44]. In contrast, our protocols in both the symmetric and standard EAPM scenarios achieve certification at significantly smaller visibilities.

Moreover, as noted in Table I, it is possible that product-measurement protocols in the symmetric EAPM scenario are fundamentally limited by some operational notion of nonclassicality that is weaker than one-way steering but stronger than entanglement. Given our results, one may be inclined to suggest that the relevant concept is usefulness in fidelity-based teleportation. However, this is not accurate because we can numerically find entanglement advantages from states with a trivial maximally entangled fraction.

Furthermore, in our protocols, Charlie always performs the product measurements. However, in practice, sometimes it can be costly to communicate the quantum messages from Alice and Bob to Charlie. We note that this can be circumvented by "splitting" Charlie into two separate parties, one neighboring Alice and one neighboring Bob, with independent inputs z and z'. By associating these inputs with the respective single-particle measurements entering Charlie's product measurement, we can recover the same statistics as in our protocols by imposing the postselection condition $z = z'$.

Another relevant discussion is that of closing the detection loophole. Our protocols have not been designed with the aim of minimizing detection requirements but they nevertheless perform well in this regard. Deterministic and complete entangled measurements on separate photons are well known to be complicated and require additional resources such as nonlinear optics or auxiliary qubits (see, e.g., Refs. [13,14,48]). This is particularly well known for the seminal Bell-state measurement [2] and it typically means that it is significantly harder to reach high total detection efficiencies with such measurements. Moreover, even implementing such measurements in dimensions larger than two is a formidable challenge. The use of protocols based on product measurements offers a clear advantage. For instance, in the symmetric EAPM scenario implemented with qubits, we require a detection efficiency per photon of roughly 57.7%. Recent Bell-inequality experiments have shown single photon detection efficiencies far above this value [49,50]. In contrast, we are not aware of any relevant two-photon Bell-state measurement implemented with an efficiency close to this value. Notably, the theoretical efficiency per photon needed in entanglement certification via dense coding is the same as in our protocol in the symmetric EAPM scenario. Furthermore, due to the dimensional scalability of product measurements, both Proposition 1 and Conjecture 1 suggest that the advantages in detection efficiency are even more significant for larger dimensions, as the efficiency threshold per photon will decrease monotonically with d. For instance, recent experiments on entangled four-dimensional photons have shown detection efficiencies around 71.7% [51], well above the regime needed for protocols of our type.

APPENDIX A: PROOF OF L_d

We prove that for d-dimensional states α_x and measurements $\{M_{c|z}\}$, it holds that

$$\max_{\{\alpha_x\},\{M_{c|z}\}} \frac{1}{d^2(d+1)} \sum_{x,z} \text{tr}\left(\alpha_x M_{w_z|z}\right) \le \frac{1}{d}\left(1 + \frac{d-1}{\sqrt{d+1}}\right)$$

$$\equiv L_d. \tag{A1}$$

The proof closely parallels that used to arrive at Result 1 in Ref. [29].

Trivially reexpress the objective function on the left-hand side of Eq. (A1) as

$$\mathcal{S}_d = \frac{1}{d^2(d+1)} \sum_{x,z} \frac{1}{d} \text{tr}\left(M_{w_z|z}\right)$$

$$+ \frac{1}{d^2(d+1)} \sum_x \text{tr}\left(\alpha_x \sum_z \left(M_{w_z|z} - \frac{\mathbb{1}}{d}\text{tr}(M_{w_z|z})\right)\right). \tag{A2}$$

Note that because of the winning conditions

$$\begin{aligned} z \ne d: && w_z = x_1 - 2zx_0 \mod d \\ z = d: && w_d = x_0, \end{aligned} \tag{A3}$$

it follows that $\sum_x M_{w_z|z} = d\mathbb{1}$ for every z. Therefore, the first term in Eq. (A2) simply becomes $\frac{1}{d}$. For the second term in Eq. (A2), the optimal α_x corresponds to the largest eigenvalue of the operator $O_x = \sum_z \left(M_{w_z|z} - (\mathbb{1}/d)\text{tr}(M_{w_z|z})\right)$. Thus we have

$$\mathcal{S}_d = \frac{1}{d} + \frac{1}{d^2(d+1)} \sum_x \|O_x\|_\infty, \tag{A4}$$

where $\|\cdot\|_\infty$ is the largest modulus eigenvalue. We then use norm inequality from Ref. [29]: for any trace-zero Hermitian O, it holds that

$$\|O\|_\infty \le \sqrt{\frac{\text{rank}(O) - 1}{\text{rank}(O)}} \|O\|_F, \tag{A5}$$

where $\|O\|_F = \sqrt{\text{tr}(OO^\dagger)}$ is the Frobenius norm. Applying this to each O_x and then using the concavity of the square-root function yields

$$\mathcal{S}_d \le \frac{1}{d} + \frac{1}{d(d+1)}\sqrt{\frac{d-1}{d}}\sqrt{\sum_x \text{tr}(O_x^2)}. \tag{A6}$$

We proceed by examining $I = \sum_x \text{tr}(O_x^2)$. It becomes

$$I = \sum_x \sum_{z',z=1}^{d+1} \text{tr}(M_{w_{z'}|z'} M_{w_z|z})$$

$$- \frac{1}{d} \sum_x \sum_{z',z=1}^{d+1} \text{tr}(M_{w_{z'}|z'})\text{tr}(M_{w_z|z}). \tag{A7}$$

Label the first term I_1 and the second term I_2. We evaluate them one by one:

$$I_1 = \sum_x \sum_z \text{tr}(M_{w_z|z}^2) + \sum_x \sum_{z' \ne z} \text{tr}(M_{w_{z'}|z'} M_{w_z|z}). \tag{A8}$$

Consider the second term. For a given pair (z', z), we can define the set $T_{z',z}^c$ as the set of all pairs (x_0, x_1) such that $w_{z'} = c$. (i) When $z' = d$, characterizing $T_{z',z}^c$ is trivial, since its elements simply correspond to the pairs $\{(c = x_0, x_1)\}_{x_1}$. It is easily seen that $\{T_{z',z}^c\}_{c=0}^{d-1}$ is a partition of the set of all pairs (x_0, x_1). (ii) When $z' \ne d$ and $z = d$, we let $T_{z',z}^c$ correspond to all pairs (x_0, x_1), where $x_0 = (2z')^{-1}(x_1 - c)$. Note that the modular inverse always exists and is unique when d is prime. $\{T_{z',z}^c\}_{c=0}^{d-1}$ is a partition of the set of all pairs (x_0, x_1). (iii) When $z' \ne d$ and $z \ne d$, the elements of $T_{z',z}^c$ correspond to choosing $x_0 = (2z')^{-1}(x_1 - c)$ for $x_1 \in \{0, \ldots, d-1\}$. This gives $w_z = x_1\left(1 - 2z(2z')^{-1}\right) + 2z(2z')^{-1}c$. Again, $\{T_{z',z}^c\}_{c=0}^{d-1}$ is a partition of the set of all pairs (x_0, x_1).

Over all three cases, it holds that for every (z', z, c),

$$\sum_{x \in T_{z',z}^c} M_{w_z|z} = \mathbb{1}. \tag{A9}$$

Thus, we can write

$$\sum_x \sum_{z' \ne z} \text{tr}(M_{w_{z'}|z'} M_{w_z|z}) = \sum_{z' \ne z} \sum_{c=0}^{d-1} \sum_{x \in T_{z',z}^c} \text{tr}(M_{w_{z'}|z'} M_{w_z|z})$$

$$= \sum_{z' \ne z} \sum_{c=0}^{d-1} \text{tr}\left(M_{c|z'} \sum_{x \in T_{z',z}^c} M_{w_z|z}\right)$$

$$= \sum_{z' \ne z} \sum_{c=0}^{d-1} \text{tr}(M_{c|z'})$$

$$= d \sum_{z' \ne z} = d^2(d+1). \tag{A10}$$

In the first step, we have used that $T_{z',z}^c$ is a partition of the set of x. In the second step, we use that $w_{z'} = c$ for every

$x \in T^c_{z',z}$. In the third step, we use Eq. (A9) when $(z',z) \neq d$ and similarly when either $z' = d$ or $z = d$. Thus, we have

$$I_1 = \sum_x \sum_z \text{tr}(M^2_{w_z|z}) + d^2(d+1). \quad (A11)$$

Similarly, for the term I_2, we obtain the lower bound

$$I_2 \geq \frac{1}{d} \sum_x \sum_z \text{tr}(M^2_{w_z|z}) + \frac{1}{d} \sum_x \sum_{z'\neq z} \text{tr}(M_{w_{z'}|z'})\text{tr}(M_{w_z|z}). \quad (A12)$$

Again using the partition $\{T^c_{z',z}\}_c$ for the set of x, the second term reduces to becomes $d^2(d+1)$.

Inserting the above back into Eq. (A7), we obtain

$$I \leq \frac{d-1}{d} \sum_x \sum_z \text{tr}(M^2_{w_z|z}) \leq \frac{d-1}{d} \sum_x \sum_z \text{tr}(M_{w_z|z})$$
$$= d(d^2-1). \quad (A13)$$

Inserting this into Eq. (A6), we obtain the final result:

$$\mathcal{S}_d \leq \frac{1}{d} + \frac{d-1}{d\sqrt{d+1}}. \quad (A14)$$

APPENDIX B: QUBIT BALANCED XOR SCHEMES

We consider the case of qubit communication ($d = 2$) in the symmetric EAPM scenario. We allow Alice, Bob, and Charlie to have arbitrary inputs, with alphabet sizes N_X, N_Y, and N_Z inputs each. Charlie's output is binary, $c \in \{0, 1\}$. In general, for each z, Charlie is tasked with outputting the value of some function of Alice's and Bob's inputs, $c = f_z(x,y)$. Its average success rate is

$$\mathcal{W} = \frac{1}{N_X N_Y N_Z} \sum_{x,y,z} p(c = f_z(x,y)|x,y,z). \quad (B1)$$

We focus on the broad class of schemes in which the winning condition is an XOR game with balanced functions, i.e., any choice of $f_z(x,y)$ such that

$$f_z(x,y) = g_z(x) + h_z(y) \quad \text{mod } 2, \quad (B2)$$

for some arbitrary functions g_z and h_z that are balanced. Recall that a function $u : \{1,\ldots,M\} \rightarrow \{0,1\}$ is called balanced if half the domain is mapped to 0 and the other half is mapped to 1. This means that N_X and N_Y must be even numbers.

We now derive an upper bound on $\mathcal{W}$ for any quantum model without shared entanglement. In such models, the average success rate reads

$$\mathcal{W} = \frac{1}{N_X N_Y N_Z} \sum_{c,x,y,z} \text{tr}\left(\alpha_x \otimes \beta_y M_{c|z}\right) \delta_{c,f_z(x,y)}. \quad (B3)$$

Using the normalization $M_{0|z} + M_{1|z} = \mathbb{1}$, we can express this as

$$\mathcal{W} = \frac{1}{2} + \frac{1}{N_X N_Y N_Z} \sum_{x,y,z} (-1)^{f_z(x,y)} \text{tr}\left(\alpha_x \otimes \beta_y M_{0|z}\right). \quad (B4)$$

Using that $f_z(x,y) = g_z(x) + h_z(y)$, we rearrange this as

$$\mathcal{W} = \frac{1}{2} + \frac{1}{N_X N_Y N_Z} \sum_z \text{tr}\left(M_{0|z} O^A_z \otimes O^B_z\right), \quad (B5)$$

where

$$O^A_z = \sum_x (-1)^{g_z(x)} \alpha_x, \quad (B6)$$

$$O^B_z = \sum_y (-1)^{h_z(y)} \beta_y. \quad (B7)$$

The optimal choice of $M_{0|z}$ is the projector onto the positive eigenspace of the operator $O^A_z \otimes O^B_z$. Thus, the optimal value of the above trace is the sum of the positive eigenvalues of $O^A_z \otimes O^B_z$. Note that since g_z and h_z are balanced, $\text{tr}(O^A_z) = \text{tr}\left(O^B_z\right) = 0$. Together with the fact that O^A_z and O^B_z are 2×2 Hermitian operators, it follows that their two respective eigenvalues have the same magnitude and opposite sign, i.e., $\lambda_1(O^A_z) = -\lambda_2(O^A_z)$ and $\lambda_1(O^B_z) = -\lambda_2(O^B_z)$, where λ_1 denotes the positive eigenvalue. Hence, the sum of positive eigenvalues of $O^A_z \otimes O^B_z$ becomes $\lambda_1(O^A_z)\lambda_1(O^B_z) + \lambda_2(O^A_z)\lambda_2(O^B_z) = 2\lambda_1(O^A_z)\lambda_1(O^B_z)$. Hence,

$$\mathcal{W} \leq \frac{1}{2} + \frac{2}{N_X N_Y N_Z} \sum_z \lambda_1(O^A_z)\lambda_1(O^B_z).$$

We can now use the Bloch-vector formalism to write $\alpha_x = (\mathbb{1} + \vec{\alpha}_x \cdot \vec{\sigma})/2$ and $\beta_y = (\mathbb{1} + \vec{\beta}_y \cdot \vec{\sigma})/2$, where $\vec{\sigma} = (\sigma_X, \sigma_Y, \sigma_Z)$, for some unit vectors $\{\vec{\alpha}_x\}$ and $\{\vec{\beta}_y\}$ in $\mathbb{R}^3$. We can now write $O^A_z = \frac{1}{2}\vec{a}_z \cdot \vec{\sigma}$ and $O^B_z = \frac{1}{2}\vec{b}_z \cdot \vec{\sigma}$, where we have defined the unnormalized vectors $\vec{a}_z = \sum_x (-1)^{g_z(x)}\vec{\alpha}_x$ and $\vec{b}_z = \sum_y (-1)^{h_z(x)}\vec{\beta}_y$. It is easily shown that the eigenvalues of an operator $\vec{n} \cdot \vec{\sigma}$ are $\pm|\vec{n}|$. Thus, we

arrive at

$$\mathcal{W} \leq \frac{1}{2} + \frac{1}{2N_X N_Y N_Z} \sum_z |\vec{a}_z||\vec{b}_z|$$

$$\leq \frac{1}{2} + \frac{1}{2N_X N_Y N_Z} \sqrt{\sum_z |\vec{a}_z|^2} \sqrt{\sum_z |\vec{b}_z|^2}, \quad \text{(B8)}$$

where in the second line we have used the Cauchy-Schwarz inequality. This has the advantage that we can now consider the optimization problem separately for each square-root factor. The expressions under the square roots can be expanded to $\sum_z |\vec{a}_z|^2 = N_X N_Z + 2\eta$ and $\sum_z |\vec{b}_z|^2 = N_Y N_Z + 2\xi$, where

$$\eta \equiv \sum_{x < x'} \vec{\alpha}_x \cdot \vec{\alpha}_{x'} \sum_z (-1)^{g_z(x) + g_z(x')} \quad \text{(B9)}$$

$$\xi \equiv \sum_{y < y'} \vec{\beta}_y \cdot \vec{\beta}_{y'} \sum_z (-1)^{h_z(y) + h_z(y')}. \quad \text{(B10)}$$

Thus, one is left with optimizing these two expressions independently. One possible way of doing this is to define the Gram matrix $G_{x,x'} = \alpha_x \cdot \alpha_{x'}$. Note that this matrix is, by construction, both symmetric ($G = G^T$) and positive semidefinite ($G \succeq 0$). In addition, its diagonal elements are unit ($G_{xx} = 1$). Hence, we can relax our optimization of η to the semidefinite program

$$\tilde{\eta} = \max_G \quad \sum_{x < x'} G_{x,x'} \left(\sum_z (-1)^{g_z(x) + g_z(x')} \right)$$

$$\text{such that} \quad G \succeq 0, \qquad G = G^T, \qquad G_{xx} = 1 \quad \forall x \quad \text{(B11)}$$

Similarly, we can define a Gram matrix over the Bloch vectors $\{\vec{\beta}_y\}$ and bound ξ by the analogous semidefinite program

$$\tilde{\xi} = \max_G \quad \sum_{y < y'} G_{y,y'} \left(\sum_z (-1)^{h_z(y) + h_z(y')} \right)$$

$$\text{such that} \quad G \succeq 0, \qquad G = G^T, \qquad G_{yy} = 1 \quad \forall y. \quad \text{(B12)}$$

Thus, we can systematically compute bounds of the form

$$\mathcal{W} \leq \frac{1}{2} + \frac{1}{2N_X N_Y N_Z} \sqrt{N_X N_Z + 2\tilde{\eta}} \sqrt{N_Y N_Z + 2\tilde{\xi}}. \quad \text{(B13)}$$

We now apply this to the specific scheme considered in the main text, i.e., the quantity $\mathcal{R}_2$. Clearly, the symmetry between Alice and Bob means $\tilde{\eta} = \tilde{\xi}$. Moreover, for the above semidefinite program, all coefficients appearing in

front of the Gram matrix in the objective function are -1. Therefore, the program is invariant under permutations of the label x. Therefore, the semidefinite program simplifies to

$$\tilde{\eta} = \max \quad -6u$$

$$\text{such that} \quad \begin{pmatrix} 1 & u & u & u \\ u & 1 & u & u \\ u & u & 1 & u \\ u & u & u & 1 \end{pmatrix} \succeq 0. \quad \text{(B14)}$$

As the distinct eigenvalues of the matrix are $1 - u$ and $1 + 3u$, it follows that the optimal choice is $u = -\frac{1}{3}$ and thus $\tilde{\eta} = 2$. Inserting this into Eq. (B13), we obtain $\mathcal{R}_2 \leq \frac{2}{3}$.

APPENDIX C: CONNECTION WITH QUBIT MAXIMALLY ENTANGLED FRACTION

Here, we would like to prove that Proposition 2 in Sec. V is tight for shared arbitrary *pure* states. To this end, we find an upper bound that is equal to Eq. (23).

First, note that any two-qubit pure state can be written in its Schmidt decomposition as

$$|\Psi_{AB}(\theta)\rangle = \cos\theta |\psi_A, \psi_B\rangle + \sin\theta |\psi_A^\perp, \psi_B^\perp\rangle$$

$$= V^A \otimes V^B (\cos\theta |0_A, 0_B\rangle + \sin\theta |1_A, 1_B\rangle)$$

$$= V^A \otimes V^B |\Phi_{AB}(\theta)\rangle, \quad \text{(C1)}$$

where $\{\psi_\gamma, \psi_\gamma^\perp\}$ represent an arbitrary orthogonal bases for the party $\gamma \in \{A, B\}$, V^γ is a local unitary acting on the same Hilbert space, and $\theta \in [0, \pi/4]$. One can show that the maximally entangled fraction of such a state is independent of the local unitaries and only determined by θ:

$$\text{EF}_2 := \text{EF}_2(\Psi_{AB}(\theta)) = \frac{1}{2}(1 + \sin 2\theta). \quad \text{(C2)}$$

Second, take the same arbitrary state $\Psi_{AB}(\theta)$ given in Eq. (C1). Upon the application of local channels Λ_x^A (Λ_y^B) by Alice (Bob) and the measurement $M_{c|z}$ by Charlie—not necessarily separable—the winning score reads

$$\mathcal{R}_2 = \frac{1}{48} \sum_{x,y,z} \text{tr}\left((\tilde{\Lambda}_x^A \otimes \tilde{\Lambda}_y^B) [\Phi_{AB}(\theta)] M_{f_z(x,y)|z} \right). \quad \text{(C3)}$$

where we have also absorbed the local unitaries V^γ into the local channels such that $\tilde{\Lambda}_\alpha^\gamma[\bullet] = \Lambda_\alpha^\gamma[V^\gamma \bullet V^{\gamma\dagger}]$—since Alice and Bob have the chance to optimize their local operations anyway. The average score rates can be further

simplified to

$$\mathcal{R}_2 = \frac{1}{2} + \frac{1}{48} \sum_{x,y,z} \mathrm{tr}\left((-1)^{f_z(x,y)}(\tilde{\Lambda}_x^A \otimes \tilde{\Lambda}_y^B)[\Phi_{AB}(\theta)] M_{0|z}\right).$$

(C4)

Next, note that the shared state $\Phi_{AB}(\theta)$ can be expressed in terms of Pauli matrices:

$$\begin{aligned}\Phi_{AB}(\theta) = &\frac{\cos^2\theta}{4}(\mathbb{1} + \sigma_3) \otimes (\mathbb{1} + \sigma_3) \\ &+ \frac{\sin^2\theta}{4}(\mathbb{1} - \sigma_3) \otimes (\mathbb{1} - \sigma_3) \\ &+ \frac{\sin 2\theta}{4}(\sigma_1 \otimes \sigma_1 - \sigma_2 \otimes \sigma_2).\end{aligned}$$

(C5)

Furthermore, since $\tilde{\Lambda}_\alpha$ is a quantum channel, for any arbitrary Bloch vector $\vec{m}$ with $|\vec{m}| \leq 1$, we should have

$$\tilde{\Lambda}_\alpha\left[\frac{1}{2}(\mathbb{1} + \vec{m} \cdot \vec{\sigma})\right] = \frac{1}{2}(\mathbb{1} + \vec{r}_\alpha \cdot \vec{\sigma}),$$

(C6)

$$\tilde{\Lambda}_\alpha[\vec{m} \cdot \vec{\sigma}] = \vec{s}_\alpha \cdot \vec{\sigma},$$

(C7)

where $|\vec{r}_\alpha| \leq 1$—since the right-hand side of Eq. (C6) is a normalized state. Moreover, we should also have $|\vec{s}_\alpha| \leq 1$. To see this, first applying the channel to the maximally mixed state yields $\tilde{\Lambda}_\alpha[\mathbb{1}/2] = \frac{1}{2}(\mathbb{1} + \vec{r}_\alpha^0 \cdot \vec{\sigma})$ for some $|\vec{r}_\alpha^0| \leq 1$. Next, take two density matrices $\varrho_\pm = \frac{1}{2}(\mathbb{1} \pm \vec{m} \cdot \vec{\sigma})$ and apply the channel to them. The linearity of the channel dictates that

$$\tilde{\Lambda}_\alpha[\varrho_\pm] = \tilde{\Lambda}_\alpha\left[\frac{\mathbb{1}}{2}\right] \pm \frac{1}{2}\tilde{\Lambda}_\alpha[\vec{m} \cdot \vec{\sigma}] = \frac{\mathbb{1}}{2} + \frac{1}{2}(\vec{r}_\alpha^0 \pm \vec{s}_\alpha) \cdot \vec{\sigma}.$$

Now, if $|\vec{s}_\alpha| > 1$, at least one of the two vectors $\vec{r}_\alpha^0 \pm \vec{s}_\alpha$ has a norm above one, which contradicts the physicality of the channel. Thus we should always have $|\vec{s}_\alpha| \leq 1$.

Applying the local channels to $\Phi_{AB}(\theta)$ gives

$$\begin{aligned}&(\tilde{\Lambda}_x^A \otimes \tilde{\Lambda}_y^B)[\Phi_{AB}(\theta)] \\ &= \frac{\cos^2\theta}{4}(\mathbb{1} + \vec{m}_x^1 \cdot \vec{\sigma}) \otimes (\mathbb{1} + \vec{n}_y^1 \cdot \vec{\sigma}) \\ &+ \frac{\sin^2\theta}{4}(\mathbb{1} + \vec{m}_x^2 \cdot \vec{\sigma}) \otimes (\mathbb{1} + \vec{n}_y^2 \cdot \vec{\sigma}) \\ &+ \frac{\sin 2\theta}{4}(\vec{m}_x^3 \cdot \vec{\sigma} \otimes \vec{n}_y^3 \cdot \vec{\sigma} + \vec{m}_x^4 \cdot \vec{\sigma} \otimes \vec{n}_y^4 \cdot \vec{\sigma}),\end{aligned}$$

(C8)

for some vectors $\{\vec{m}_x^k, \vec{n}_y^k\}_{k=1}^4$ that satisfy $|\vec{m}_x^k| \leq 1$ and $|\vec{n}_y^k| \leq 1$—note that we have absorbed a minus sign in the vector $\vec{m}_x^4$. By plugging into Eq. (C4) and noting that

$f_z(x,y) = g_z(x) + h_z(y) \mod 2$, with balanced functions $g_z(x)$ and $h_z(y)$, we have

$$\begin{aligned}\mathcal{R}_2 = &\frac{1}{2} + \frac{1}{48} \\ &\times \sum_{x,y,z} \sum_{i=1}^4 \tau_i \, \mathrm{tr}\left((-1)^{g_z(x)+h_z(y)} \vec{m}_x^i \cdot \vec{\sigma} \otimes \vec{n}_y^i \cdot \vec{\sigma} M_{0|z}\right),\end{aligned}$$

(C9)

where $\tau = \frac{1}{4}(\cos^2(\theta), \sin^2(\theta), \sin 2\theta, \sin 2\theta) \geq 0$ within the domain of θ. We have also made use of the fact that for any balanced function $f(x)$, $\sum_x(-1)^{f(x)} = 0$.

We can bring $\mathcal{R}_2$ to a similar form as Eq. (B5),

$$\mathcal{R}_2 = \frac{1}{2} + \frac{1}{12} \sum_{i=1}^4 \tau_i \sum_z \mathrm{tr}\left(M_{0|z} O_{z,i}^A \otimes O_{z,i}^B\right),$$

(C10)

where

$$O_{z,i}^A = \frac{1}{2} \sum_x (-1)^{g_z(x)} \vec{m}_x^i \cdot \vec{\sigma},$$

(C11)

$$O_{z,i}^B = \frac{1}{2} \sum_y (-1)^{h_z(y)} \vec{n}_y^i \cdot \vec{\sigma}.$$

(C12)

One can separately bound each of the four terms by using the result obtained in Appendix B—see Eqs. (B13) and (B14)—to obtain

$$\sum_z \mathrm{tr}\left(M_{0|z} O_{z,i}^A \otimes O_{z,i}^B\right) \leq 8,$$

(C13)

which is independent of "i." Therefore,

$$\mathcal{R}_2 \leq \frac{1}{2} + \frac{2}{3} \sum_{i=1}^4 \tau_i = \frac{1}{3} + \frac{2}{3} \mathrm{EF}_2(\theta).$$

(C14)

where we have used Eq. (C2) to evaluate $\sum_{i=1}^4 \tau_i = \mathrm{EF}_2(\theta) - \frac{1}{4}$.

APPENDIX D: CONNECTION WITH MAXIMALLY ENTANGLED FRACTION FOR ARBITRARY d

First, we prove that $\mathcal{R}_d = 1$. For simplicity, we define the projector $E_{m|z} = |e_{m,z}\rangle\langle e_{m,z}|$. We measure one particle in the basis $\{E_{c_1|z}\}$, with outcome c_1, and the other particle in the conjugated basis $\{E_{c_2|z}^*\}$, with outcome c_2. The final output is defined as $c = c_1 - c_2 \mod d$. Thus, the positive operator-valued measure describing this measurement

becomes

$$M_{c|z} = \sum_{c_1,c_2} E_{c_1|z} \otimes E^*_{c_2|z} \delta_{c,c_1-c_2}. \quad (D1)$$

Next, via a direct calculation, it is possible to show these relations (given in the main text) for any $z = 0, \ldots, d - 1$:

$$\begin{aligned}
X^t|e_{m,z}\rangle &= \omega^{zt^2-tm}|e_{m-2zt,z}\rangle, \\
X^t|e^*_{m,z}\rangle &= \omega^{-zt^2+tm}|e^*_{m-2zt,z}\rangle, \\
Z^t|e_{m,z}\rangle &= |e_{m+t,z}\rangle, \\
Z^t|e^*_{m,z}\rangle &= |e^*_{m-t,z}\rangle.
\end{aligned} \quad (D2)$$

That is, applying any unitary of the form $X^{t_1}Z^{t_2}$ to any of the eigenstates associated with the first d bases are mapped into other eigenstates of the same basis. In other words, the basis $\{|e_{m,z}\rangle\}_{m=1}^{d}$ is closed under the operation of $X^{t_1}Z^{t_2}$ for $z = 0, \ldots, d - 1$.

Now consider the probability of outputting the right answer, $c = w_z$, for $z = 0, \ldots, d - 1$. It reads

$$\begin{aligned}
&p(c = w_z|x,y,z) \\
&= \sum_{c_1} \langle\phi_d^+| \left(|v_{c_1xz}\rangle\langle v_{c_1xz}| \otimes |\mu_{c_1xyz}\rangle\langle\mu_{c_1xyz}|\right) |\phi_d^+\rangle,
\end{aligned} \quad (D3)$$

where

$$|v_{c_1xz}\rangle = Z^{-x_1}X^{-x_0}|e_{c_1,z}\rangle, \quad (D4)$$

$$|\mu_{c_1xyz}\rangle = Z^{-y_1}X^{-y_0}|e^*_{c_1-w_z,z}\rangle. \quad (D5)$$

Successively applying the relations in Eq. (D2), one finds that

$$\begin{aligned}
|v_{c_1xz}\rangle\langle v_{c_1xz}| &= E_{c_1+2zx_0-x_1|z} \\
|\mu_{c_1xyz}\rangle\langle\mu_{c_1xyz}| &= E^*_{c_1+2zx_0-x_1|z}.
\end{aligned} \quad (D6)$$

Note that the second vector now has no dependence on y. From the relation, $\mathbb{1} \otimes O|\phi_d^+\rangle = O^T \otimes \mathbb{1}|\phi_d^+\rangle$ and the fact that $\{E_{m|z}\}$ forms a orthonormal basis, it follows that

$$p(w_z|x,y,z) = \frac{1}{d}\sum_{c_1} \text{Tr}\left(E_{c_1+2zx_0-x_1|z}E_{c_1+2zx_0-x_1|z}\right) = 1. \quad (D7)$$

Performing the same calculation for the computational basis, $z = d$, gives an analogous result. Hence, we have perfect correlations for every z and hence we achieve the algebraically optimal value $\mathcal{R}_d = 1$.

The maximally entangled fraction is defined as

$$\text{EF}_d(\rho) = \max_{\Lambda_1,\Lambda_2} \langle\phi^+|(\Lambda_1 \otimes \Lambda_2)[\rho]|\phi_d^+\rangle, \quad (D8)$$

where Λ_1 and Λ_2 are CPTP maps with d-dimensional output spaces. If it exceeds $1/d$, the state is entangled. To show that this quantity is relevant for the value of $\mathcal{R}_d$, let Alice and Bob first apply local CPTP maps Λ_1 and Λ_2, respectively, before applying the protocol used above to arrive at $\mathcal{R}_d = 1$ for the maximally entangled state.

We can write the figure of merit as

$$\mathcal{R}_d = \frac{1}{d+1}\text{tr}\left((\Lambda_1 \otimes \Lambda_2)[\rho]\sum_{z=0}^{d}\mathcal{R}_d^{(z)}\right), \quad (D9)$$

where we have defined

$$\mathcal{R}_d^{(z)} = \frac{1}{d^4}\sum_{x,y,c_1} |v_{c_1xz}\rangle\langle v_{c_1xz}| \otimes |\mu_{c_1xyz}\rangle\langle\mu_{c_1xyz}| \quad (D10)$$

for $z = 0, \ldots, d - 1$. Using Eq. (D6) and taking the sums over (x, y, c_1), we obtain

$$\mathcal{R}_d^{(z)} = \sum_{c=0}^{d-1} E_{c|z} \otimes E^*_{c|z}. \quad (D11)$$

This can be thought of as an unnormalized correlated-coin state in the zth MUB. Indeed, a direct calculation for the computational basis—namely, $z = d$—analogously leads to $\mathcal{R}_d^{(d)} = \sum_{c=0}^{d-1} |cc\rangle\langle cc|$. Now, we can use the key fact that for any complete set of mutually unbiased bases, it holds that [42]

$$\mathcal{T} \equiv \sum_{z=0}^{d}\sum_{c=0}^{d-1} E_{c|z} \otimes E^*_{c|z} = \mathbb{1} + d\phi_d^+. \quad (D12)$$

Hence, we have

$$\begin{aligned}
\mathcal{R}_d &= \frac{1}{d+1}\text{tr}\left((\Lambda_1 \otimes \Lambda_2)[\rho]\mathcal{T}\right) \\
&= \frac{1}{d+1} + \frac{d}{d+1}\text{tr}\left((\Lambda_1 \otimes \Lambda_2)[\rho]\phi_d^+\right).
\end{aligned} \quad (D13)$$

Since we can allow any channels for Alice and Bob, we can choose those that correspond to the maximally entangled fraction of ρ. Hence, we have obtained

$$\mathcal{R}_d = \frac{1}{d+1} + \frac{d}{d+1}\text{EF}_d(\rho). \quad (D14)$$

[1] C. H. Bennett and S. J. Wiesner, Communication via one- and two-particle operators on Einstein-Podolsky-Rosen states, Phys. Rev. Lett. **69**, 2881 (1992).

[2] N. Lütkenhaus, J. Calsamiglia, and K.-A. Suominen, Bell measurements for teleportation, Phys. Rev. A **59**, 3295 (1999).

[3] L. Vaidman and N. Yoran, Methods for reliable teleportation, Phys. Rev. A **59**, 116 (1999).

[4] P. van Loock and N. Lütkenhaus, Simple criteria for the implementation of projective measurements with linear optics, Phys. Rev. A **69**, 012302 (2004).

[5] C.-X. Huang, X.-M. Hu, Y. Guo, C. Zhang, B.-H. Liu, Y.-F. Huang, C.-F. Li, G.-C. Guo, N. Gisin, C. Branciard, and A. Tavakoli, Entanglement swapping and quantum correlations via symmetric joint measurements, Phys. Rev. Lett. **129**, 030502 (2022).

[6] Y. Guo, H. Tang, J. Pauwels, E. Z. Cruzeiro, X.-M. Hu, B.-H. Liu, Y.-F. Huang, C.-F. Li, G.-C. Guo, and A. Tavakoli, Experimental higher-dimensional entanglement advantage over qubit channel, ArXiv:2306.13495.

[7] K. Mattle, H. Weinfurter, P. G. Kwiat, and A. Zeilinger, Dense coding in experimental quantum communication, Phys. Rev. Lett. **76**, 4656 (1996).

[8] X. Fang, X. Zhu, M. Feng, X. Mao, and F. Du, Experimental implementation of dense coding using nuclear magnetic resonance, Phys. Rev. A **61**, 022307 (2000).

[9] X. Li, Q. Pan, J. Jing, J. Zhang, C. Xie, and K. Peng, Quantum dense coding exploiting a bright Einstein-Podolsky-Rosen beam, Phys. Rev. Lett. **88**, 047904 (2002).

[10] J. Jing, J. Zhang, Y. Yan, F. Zhao, C. Xie, and K. Peng, Experimental demonstration of tripartite entanglement and controlled dense coding for continuous variables, Phys. Rev. Lett. **90**, 167903 (2003).

[11] T. Schaetz, M. D. Barrett, D. Leibfried, J. Chiaverini, J. Britton, W. M. Itano, J. D. Jost, C. Langer, and D. J. Wineland, Quantum dense coding with atomic qubits, Phys. Rev. Lett. **93**, 040505 (2004).

[12] C. Schuck, G. Huber, C. Kurtsiefer, and H. Weinfurter, Complete deterministic linear optics Bell state analysis, Phys. Rev. Lett. **96**, 190501 (2006).

[13] J. T. Barreiro, T.-C. Wei, and P. G. Kwiat, Beating the channel capacity limit for linear photonic superdense coding, Nat. Phys. **4**, 282 (2008).

[14] B. P. Williams, R. J. Sadlier, and T. S. Humble, Superdense coding over optical fiber links with complete Bell-state measurements, Phys. Rev. Lett. **118**, 050501 (2017).

[15] J. Calsamiglia, Generalized measurements by linear elements, Phys. Rev. A **65**, 030301 (2002).

[16] X.-M. Hu, C. Zhang, B.-H. Liu, Y. Cai, X.-J. Ye, Y. Guo, W.-B. Xing, C.-X. Huang, Y.-F. Huang, C.-F. Li, and G.-C. Guo, Experimental high-dimensional quantum teleportation, Phys. Rev. Lett. **125**, 230501 (2020).

[17] Y.-H. Luo, H.-S. Zhong, M. Erhard, X.-L. Wang, L.-C. Peng, M. Krenn, X. Jiang, L. Li, N.-L. Liu, C.-Y. Lu, A. Zeilinger, and J.-W. Pan, Quantum teleportation in high dimensions, Phys. Rev. Lett. **123**, 070505 (2019).

[18] X.-M. Hu, Y. Guo, B.-H. Liu, Y.-F. Huang, C.-F. Li, and G.-C. Guo, Beating the channel capacity limit for superdense coding with entangled ququarts, Sci. Adv. **4**, eaat9304 (2018).

[19] A. Tavakoli, J. Pauwels, E. Woodhead, and S. Pironio, Correlations in entanglement-assisted prepare-and-measure scenarios, PRX Quantum **2**, 040357 (2021).

[20] J. Pauwels, A. Tavakoli, E. Woodhead, and S. Pironio, Entanglement in prepare-and-measure scenarios: Many questions, a few answers, New J. Phys. **24**, 063015 (2022).

[21] C. Vieira, C. de Gois, L. Pollyceno, and R. Rabelo, Interplays between classical and quantum entanglement-assisted communication scenarios, ArXiv:2205.05171.

[22] J. Pauwels, S. Pironio, E. Z. Cruzeiro, and A. Tavakoli, Adaptive advantage in entanglement-assisted communications, Phys. Rev. Lett. **129**, 120504 (2022).

[23] A. Piveteau, J. Pauwels, E. Håkansson, S. Muhammad, M. Bourennane, and A. Tavakoli, Entanglement-assisted quantum communication with simple measurements, Nat. Commun. **13**, 7878 (2022).

[24] A. Tavakoli, A. A. Abbott, M.-O. Renou, N. Gisin, and N. Brunner, Semi-device-independent characterization of multipartite entanglement of states and measurements, Phys. Rev. A **98**, 052333 (2018).

[25] G. Moreno, R. Nery, C. de Gois, R. Rabelo, and R. Chaves, Semi-device-independent certification of entanglement in superdense coding, Phys. Rev. A **103**, 022426 (2021).

[26] W. K. Wootters and B. D. Fields, Optimal state-determination by mutually unbiased measurements, Ann. Phys. (NY) **191**, 363 (1989).

[27] A. Ambainis, A. Nayak, A. Ta-Shma, and U. Vazirani, in *Proceedings of the Thirty-First Annual ACM Symposium on Theory of Computing*, STOC '99 (Association for Computing Machinery, New York, 1999), p. 376.

[28] A. Tavakoli, A. Hameedi, B. Marques, and M. Bourennane, Quantum random access codes using single d-level systems, Phys. Rev. Lett. **114**, 170502 (2015).

[29] M. Farkas, N. Miklin, and A. Tavakoli, Simple and general bounds on quantum random access codes, ArXiv:2312.14142.

[30] A. Tavakoli, D. Rosset, and M.-O. Renou, Enabling computation of correlation bounds for finite-dimensional quantum systems via symmetrization, Phys. Rev. Lett. **122**, 070501 (2019).

[31] M. Horodecki, P. Horodecki, and R. Horodecki, Separability of mixed states: Necessary and sufficient conditions, Phys. Lett. A **223**, 1 (1996).

[32] J. Bavaresco, M. T. Quintino, L. Guerini, T. O. Maciel, D. Cavalcanti, and M. T. Cunha, Most incompatible measurements for robust steering tests, Phys. Rev. A **96**, 022110 (2017).

[33] M. Marciniak, A. Rutkowski, Z. Yin, M. Horodecki, and R. Horodecki, Unbounded violation of quantum steering inequalities, Phys. Rev. Lett. **115**, 170401 (2015).

[34] S. Designolle, P. Skrzypczyk, F. Fröwis, and N. Brunner, Quantifying measurement incompatibility of mutually unbiased bases, Phys. Rev. Lett. **122**, 050402 (2019).

[35] H. M. Wiseman, S. J. Jones, and A. C. Doherty, Steering, entanglement, nonlocality, and the Einstein-Podolsky-Rosen paradox, Phys. Rev. Lett. **98**, 140402 (2007).

[36] A. Piveteau, A. A. Abbott, S. Muhammad, M. Bourennane, and A. Tavakoli, Weak entanglement improves quantum communication using only product measurements, ArXiv:2303.07907.

[37] Note that the qubit isotropic state is, up to local unitaries, equivalent to the qubit Werner state.

[38] M. Horodecki, P. Horodecki, and R. Horodecki, General teleportation channel, singlet fraction, and quasidistillation, Phys. Rev. A **60**, 1888 (1999).

[39] A. Tavakoli, A. Pozas-Kerstjens, P. Brown, and M. Araújo, Semidefinite programming relaxations for quantum correlations, ArXiv:2307.02551.

[40] P. Skrzypczyk and D. Cavalcanti, *Semidefinite Programming in Quantum Information Science* (IOP Publishing, Bristol, UK, 2023), pp. 2053–2563.

[41] D. Rosset, R. Ferretti-Schöbitz, J.-D. Bancal, N. Gisin, and Y.-C. Liang, Imperfect measurement settings: Implications for quantum state tomography and entanglement witnesses, Phys. Rev. A **86**, 062325 (2012).

[42] S. Morelli, M. Huber, and A. Tavakoli, Resource-efficient high-dimensional entanglement detection via symmetric projections, Phys. Rev. Lett. **131**, 170201 (2023).

[43] H. Cao, S. Morelli, L. A. Rozema, C. Zhang, A. Tavakoli, and P. Walther, Genuine multipartite entanglement without fully controllable measurements, ArXiv:2310.11946.

[44] S. Designolle, G. Iommazzo, M. Besançon, S. Knebel, P. Gelß, and S. Pokutta, Improved local models and new Bell inequalities via Frank-Wolfe algorithms, Phys. Rev. Res. **5**, 043059 (2023).

[45] P. Skrzypczyk and D. Cavalcanti, Loss-tolerant Einstein-Podolsky-Rosen steering for arbitrary-dimensional states: Joint measurability and unbounded violations under losses, Phys. Rev. A **92**, 022354 (2015).

[46] D. Collins, N. Gisin, N. Linden, S. Massar, and S. Popescu, Bell inequalities for arbitrarily high-dimensional systems, Phys. Rev. Lett. **88**, 040404 (2002).

[47] J. Pauwels, S. Pironio, E. Woodhead, and A. Tavakoli, Almost qudits in the prepare-and-measure scenario, Phys. Rev. Lett. **129**, 250504 (2022).

[48] Y.-H. Kim, S. P. Kulik, and Y. Shih, Quantum teleportation of a polarization state with a complete Bell state measurement, Phys. Rev. Lett. **86**, 1370 (2001).

[49] Y. Liu, Q. Zhao, M.-H. Li, J.-Y. Guan, Y. Zhang, B. Bai, W. Zhang, W.-Z. Liu, C. Wu, X. Yuan, H. Li, W. J. Munro, Z. Wang, L. You, J. Zhang, X. Ma, J. Fan, Q. Zhang, and J.-W. Pan, Device-independent quantum random-number generation, Nature **562**, 548 (2018).

[50] L. K. Shalm, Y. Zhang, J. C. Bienfang, C. Schlager, M. J. Stevens, M. D. Mazurek, C. Abellán, W. Amaya, M. W. Mitchell, M. A. Alhejji, H. Fu, J. Ornstein, R. P. Mirin, S. W. Nam, and E. Knill, Device-independent randomness expansion with entangled photons, Nat. Phys. **17**, 452 (2021).

[51] X.-M. Hu, C. Zhang, B.-H. Liu, Y. Guo, W.-B. Xing, C.-X. Huang, Y.-F. Huang, C.-F. Li, and G.-C. Guo, High-dimensional Bell test without detection loophole, Phys. Rev. Lett. **129**, 060402 (2022).